Spatial coherence of bending magnet radiation and application limit of the van Cittert–Zernike theorem

Y. Takayama and S. Kamada
KEK, 1-1 Oho, Tsukuba-shi, Ibaraki 305-0801, Japan
(Received 24 July 1998)

In this paper we discuss how the first-order spatial coherence of bending magnet radiation is determined. We present an analytical representation of the coherence and compare it with the numerical calculations based on the first principles. It is shown that if the electron-beam size is so large that some conditions are satisfied, the van Cittert–Zernike theorem can be used without any modification in the vertical and horizontal directions. The formalism presented will be useful in judging whether or not the electron-beam size in the storage ring can be estimated directly from the van Cittert–Zernike theorem using the synchrotron radiation interferometer. [S1063-651X(99)02106-6]

PACS number(s): 29.27.Fh, 41.60.Ap

I. INTRODUCTION

Measurement of electron-beam emittance in an electron storage ring is one of the most important themes in accelerator physics. Low emittance rings have been constructed in order to obtain high brightness at light sources and high luminosity at colliders. Accurate measurement of emittance is extremely difficult in very low emittance rings, less than 1 nm/rad in the horizontal direction, for instance.

The emittance can be determined by measuring the electron beam size σ_e. The beam size and the emittance ε are related by the following equation,

$$\sigma_e = \sqrt{\beta\varepsilon + \left(\eta \frac{\Delta E_0}{E_0}\right)^2}, \tag{1}$$

where β and η are the beta function and the dispersion function at a measuring point of the electron-beam size, respectively. E_0 and ΔE_0 are the average and the standard deviation of the beam energy, respectively. β, η, E_0, and ΔE_0 can be given by calculation and/or measurement within some accuracy.

Recently, a method using a synchrotron radiation (SR) interferometer has been under development to estimate the electron-beam size, which measures the spatial coherence of the bending magnet radiation in the visible light region [1]. The present paper intends to give the theoretical justification for and limitations of the method of estimating the electron-beam size from the spatial coherence of the bending magnet radiation.

For ordinary incoherent lights, the van Cittert–Zernike theorem can be used to calculate the spatial coherence. The theorem represents the spatial coherence as in the following for the far-field limit where the radiation field is regarded as a spherical wave [2–4], which is

$$\gamma(\boldsymbol{D}) = \frac{\int dS(\boldsymbol{x}) I(\boldsymbol{x}) \dfrac{\exp[ik(r_1 - r_2)]}{r_1 r_2}}{\sqrt{\int dS(\boldsymbol{x}) \dfrac{I(\boldsymbol{x})}{r_1} \int dS(\boldsymbol{x}) \dfrac{I(\boldsymbol{x})}{r_2}}} \simeq \frac{\int dS(\boldsymbol{x}) I(\boldsymbol{x}) \exp\left(\dfrac{ik\boldsymbol{x}\cdot\boldsymbol{D}}{L}\right)}{\int dS(\boldsymbol{x}) I(\boldsymbol{x})}, \tag{2}$$

where $\boldsymbol{k}$, $\boldsymbol{D} = \boldsymbol{Q}_1 - \boldsymbol{Q}_2$, and L are the wave-number vector of light, the distance of two observation points, and the distance between the light source and the plane where the coherence is measured, respectively. As shown in Fig. 1, we define $r_1 = |\boldsymbol{Q}_1 - \boldsymbol{x}|$ and $r_2 = |\boldsymbol{Q}_2 - \boldsymbol{x}|$, which are the distances from a point on the light source to two observation points. $I(\boldsymbol{x})$ is the distribution of light intensity on the surface of the light source and the integration is performed on the whole surface. Equation (2) denotes that the spatial coherence at the far point is given by the Fourier transformation of the intensity

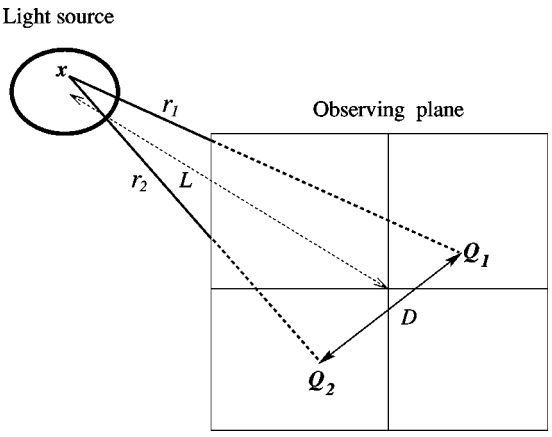

FIG. 1. The arrangement to apply the van Cittert–Zernike theorem.

distribution of the light source. In other words, the intensity distribution of the light source is estimated by measuring the spatial coherence $\gamma(\boldsymbol{D})$.

In the case of the synchrotron radiation, radiation is generated by a charge moving with nearly the speed of light and emission of light occurs along the trajectory of the moving charge rather than at the surface of the light source. Accordingly, the van Cittert–Zernike theorem must be modified to take into account this fact and the surface integration in Eq. (2) will be replaced by the integration over the phase space, which represents the trajectories of moving charges of a beam.

To answer the question of whether the van Cittert–Zernike theorem is available for the bending magnet radiation, which is raised by the recent experiment involving the SR interferometer, one needs to build an extended formula to calculate the spatial coherence of the bending magnet radiation. Historically, calculation of the bending magnet radiation was first performed by Schwinger [5]. The coherence of the synchrotron radiation has been discussed in several papers rather qualitatively [6–8] and numerical calculations of the spatial coherence of the undulator and bending magnet radiation were performed by one of the authors [9]. Based on these works, we take into account the details of the bending magnet radiation calculating the spatial coherence.

This paper consists of the following. In Sec. II, first we treat the bending magnet radiation in the time domain and describe it in terms of the wave form of the radiation field and the arrival time. In the horizontal plane on which an electron moves, the light is emitted homogeneously and the wave form is the same at any observer position on this plane, provided the distance from the emitting point to the observer is the same. The difference in the field between two observers is in the relative arrival time of the radiation. This time difference will be converted into the phase difference in the frequency domain, which plays a key roll in the spatial coherence. The phase difference in the fields will be determined by the observer position and the electron trajectory, which is a phase space position describing the initial condition of the electron's motion. The effective emitting point will be introduced to effectively measure the distance between the observer and the emitting point of radiation. It depends on the observer position and the trajectory of the electron. By conducting the above procedures, the phase of the radiation field will be given by Eqs. (28) and (29). The phase represented by Eq. (29) will violate the van Cittert–Zernike theorem expressed by the form of Eq. (2).

In the vertical plane, radiation is typically concentrated in the emission angle of $1/\gamma$, where γ is the electron energy normalized by electron rest mass and the radiation intensity decreases rapidly outside this angle. Therefore, we must take into account the wave form as well as the phase in calculating spatial coherence, both of which depend on the electron trajectory and the observer position. We will approximate the intensity distribution in the vertical direction with the Gaussian form to include this effect.

In Sec. III, the spatial coherence will be calculated using the approximated field obtained in Sec. II for the vertical and horizontal directions. We will derive the conditions under which the van Cittert–Zernike theorem is applicable. In the horizontal direction, conditions (67), (68), and (69) are obtained almost regardless of the light wavelength as long as the vertical emittance of the beam is very small. This is because the radiation is homogeneous in the horizontal direction. For the vertical direction, the conditions are given in Eqs. (79), (80), and (81). All conditions depend on the wavelength of light as well as the bending radius and the electron-beam parameters. It is because the vertical divergence of radiation is a function of the wavelength.

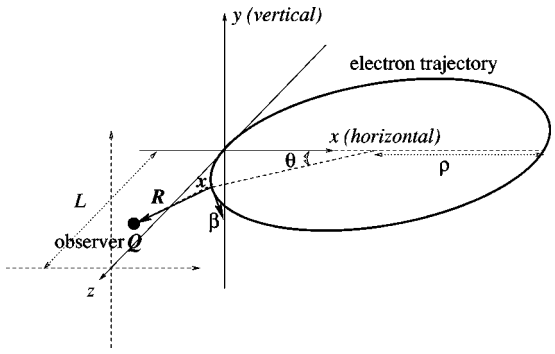

FIG. 2. Electron motion in the bending magnet. It is supposed that the electron's position and the divergence at $\theta=0$ are $(x,y,0)$ and $1/\sqrt{(1+\tan^2 x'+\tan^2 y')}(\tan x',\tan y',1)$, respectively.

In Sec. IV some numerical calculations will be conducted without any approximation in order to justify our discussions in Secs. II and III. First we calculate the spatial coherence for the beam with finite size and without divergence. In this case, the van Cittert–Zernike theorem is well satisfied in both the horizontal and vertical directions. Second, we calculate the spatial coherence for the beam with small divergence and finite size. The van Cittert–Zernike theorem is satisfied in this case, too. In these cases, the spatial coherence is determined only by the electron-beam size at the effective emitting point. Third, we calculate the coherence for the beam with large divergence, which violates the conditions derived in Sec. III. The van Cittert–Zernike theorem is found not to be applicable for this case and the spatial coherence cannot be determined only by the electron-beam size at the effective emitting point.

II. APPROXIMATION OF BENDING MAGNET RADIATION

In this section we give the trajectory of an electron in a bending magnet and the electric field emitted by it.

A single electron moves on an arc with an angular frequency ω_ρ, as shown in Fig. 2. The field of the bending magnet is assumed to have only a y component. We refer to the x and y directions as the horizontal and vertical directions, respectively. We assume that the electron passes the position $\boldsymbol{x}(\theta=0)$ with velocity $c\boldsymbol{\beta}(\theta=0)$ at time $t'=0$, where c is the light velocity and θ is defined as $\theta=\omega_\rho t'$. Then, the position and velocity of the electron at arbitrary time t' are written as

$$x(t')=\rho_0\beta_x\sin\theta+\rho_0\beta_z(1-\cos\theta)+x, \tag{3}$$

$$y(t')=\rho_0\beta_y\theta+y, \tag{4}$$

$$z(t')=\rho_0\beta_z\sin\theta-\rho_0\beta_x(1-\cos\theta)+z, \tag{5}$$

and

$$\beta_x(t')=\beta_x\cos\theta+\beta_z\sin\theta, \tag{6}$$

$$\beta_y(t')=\beta_y, \tag{7}$$

$$\beta_z(t')=\beta_z\cos(\theta)-\beta_x\sin\theta, \tag{8}$$

where we put $\rho_0=c/\omega_\rho$. We use the initial conditions,

$$\boldsymbol{x}(0)=(x,y,z), \tag{9}$$

$$\boldsymbol{\beta}(0)=(\beta_x,\beta_y,\beta_z)=\sqrt{\frac{1-\frac{1}{\gamma^2}}{1+\tan^2x'+\tan^2y'}}\,(\tan x',\tan y',1). \tag{10}$$

The electron beam has divergence x' and y' in the horizontal and vertical directions at $\theta=0$, respectively. We set the observer coordinate $\boldsymbol{Q}=(X,Y,L)$, where L is a large constant value compared with X, Y, x, and y. The bending radius ρ is given by

$$\rho=\rho_0\sqrt{\beta_x^2+\beta_z^2}\simeq\rho_0, \tag{11}$$

where we have assumed that $x',y'\ll1$.

The electric field emitted by the electron is written as [10,11]

$$\boldsymbol{E}(\boldsymbol{Q},t)=\frac{e}{4\pi\varepsilon_0}\left[\frac{1}{\kappa}\frac{\boldsymbol{n}}{R^2}+\frac{1}{c\kappa}\frac{d}{dt'}\left(\frac{\boldsymbol{n}-\boldsymbol{\beta}}{\kappa R}\right)\right]_{t=t'+R(t')/c}, \tag{12}$$

$$\boldsymbol{R}=\boldsymbol{Q}-\boldsymbol{x}(t'), \tag{13}$$

$$R=|\boldsymbol{R}|, \tag{14}$$

$$\boldsymbol{n}=\boldsymbol{R}/R, \tag{15}$$

$$\kappa=1-\boldsymbol{n}\cdot\boldsymbol{\beta}, \tag{16}$$

where e and ε_0 are the electric charge and the dielectric constant, respectively. All of the variables in the integration (12) must be evaluated at emitter time t'. An electric field with the angular frequency ω can be written as

$$\boldsymbol{E}(\boldsymbol{Q},\omega)=\frac{1}{\sqrt{2\pi}}\int dt\boldsymbol{E}(\boldsymbol{Q},t)e^{i\omega t}. \tag{17}$$

According to Eq. (12), the main contribution to the electric field comes from the short arc, where $\kappa(t')$ has the minimum value, for the high-energy electron beam. For example, if $\boldsymbol{\beta}$ and $\boldsymbol{n}$ are parallel to each other, κ becomes an extremely small value, $1/(2\gamma^2)$. The position where κ has the minimum value can be obtained by solving the equation,

$$\frac{d\kappa(t')}{dt'}=0. \tag{18}$$

The solution $t'=t'_e$ depends on the initial conditions of the electron trajectory as well as an observer position.

The observed field should have the maximum intensity at $t=t'_e+R(t'_e)/c$. Hence, we write the electric field in Eq. (12) as

$$\boldsymbol{E}(\boldsymbol{Q},t)=\boldsymbol{g}\left(\boldsymbol{Q},\boldsymbol{x},\boldsymbol{x}',\Delta E;t-t'_e-\frac{R(t'_e)}{c}\right), \tag{19}$$

where ΔE is the division of the electron-beam energy E from the central energy E_0. We redefined the two-dimensional vectors, $\boldsymbol{x}=(x,y)$ and $\boldsymbol{x}'=(x',y')$. Equations (19) and (17) are written as

$$\boldsymbol{E}(\boldsymbol{Q},\omega)=\hat{\boldsymbol{G}}(\boldsymbol{Q},\boldsymbol{x},\boldsymbol{x}',\Delta E)e^{i\Phi(\boldsymbol{Q},\boldsymbol{x},\boldsymbol{x}',\Delta E)}, \tag{20}$$

$$\Phi(\boldsymbol{Q},\boldsymbol{x},\boldsymbol{x}',\Delta E)=kR(t'_e)+\omega t'_e, \tag{21}$$

$$\hat{\boldsymbol{G}}(\boldsymbol{Q},\boldsymbol{x},\boldsymbol{x}',\Delta E)=\frac{1}{\sqrt{2\pi}}\int dt\boldsymbol{g}(\boldsymbol{Q},\boldsymbol{x},\boldsymbol{x}',\Delta E;t)e^{i\omega t}, \tag{22}$$

where $k=\omega/c$ is the wave number. Although $\hat{\boldsymbol{G}}$ and Φ depend on ω, we omit it for convenience.

Here, we make an important assumption that the phase of $\hat{\boldsymbol{G}}$ does not depend on the electron trajectory, namely, $\boldsymbol{x}$ and $\boldsymbol{x}'$, for any angular frequency ω. Moreover, we assume that the energy spread of the electron beam is so small that $\hat{\boldsymbol{G}}$ is independent of the electron energy. These assumptions make it extremely simple to calculate the spatial coherence in the following section. The physical meaning of these assumptions are important. In this case, we can put

$$\hat{G}_i(\boldsymbol{Q},\boldsymbol{x},\boldsymbol{x}',\Delta E)\equiv G_i(\boldsymbol{Q},\boldsymbol{x},\boldsymbol{x}')e^{i\chi_i(\boldsymbol{Q})}, \tag{23}$$

where $\hat{G}_i$ and G_i are the i components of vectors $\hat{\boldsymbol{G}}$ and $\boldsymbol{G}$, respectively. $\boldsymbol{G}$ and χ_i are real functions. We omit the dependence of $\boldsymbol{G}$ and χ_i on the average electron-beam energy E_0. We can regard $\boldsymbol{G}$ and Φ as the wave form and phase of the field, respectively. The phase χ_i does not affect the coherence, as shown in the following section. Since the phase χ_i is only a function of observer point $\boldsymbol{Q}$, we have

$$\frac{\hat{G}_i(\boldsymbol{Q},\boldsymbol{x},\boldsymbol{x}',\Delta E)}{\hat{G}_i(\boldsymbol{Q},\boldsymbol{0},\boldsymbol{0},0)}=\frac{G_i(\boldsymbol{Q},\boldsymbol{x},\boldsymbol{x}')}{G_i(\boldsymbol{Q},\boldsymbol{0},\boldsymbol{0})}. \tag{24}$$

Substituting Eq. (22) into Eq. (24), we have

$$\int dt\left\{g_i(\boldsymbol{Q},\boldsymbol{x},\boldsymbol{x}',\Delta E;t)-\frac{G_i(\boldsymbol{Q},\boldsymbol{x},\boldsymbol{x}')}{G_i(\boldsymbol{Q},\boldsymbol{0},\boldsymbol{0})}g_i(\boldsymbol{Q},\boldsymbol{0},\boldsymbol{0},0;t)\right\}e^{i\omega t}=0. \tag{25}$$

Since this equation is always satisfied for any angular frequency ω, we have

$$g_i(\boldsymbol{Q},\boldsymbol{x},\boldsymbol{x}',\Delta E;t)=\frac{G_i(\boldsymbol{Q},\boldsymbol{x},\boldsymbol{x}')}{G_i(\boldsymbol{Q},\boldsymbol{0},\boldsymbol{0})}g_i(\boldsymbol{Q},\boldsymbol{0},\boldsymbol{0},0;t). \tag{26}$$

According to Eq. (26), the above assumption is equivalent to the electric field being factored into the two functions, one of

which depends only on the time and observer position, and the other only on the electron trajectory and the observer position.

Next, we calculate the phase term in Eq. (21) using the following approximations:

$$X,Y,x,y \ll \rho_0, L,$$

$$x',y' \ll 1,$$

$$\frac{1}{\gamma_0} \ll 1,$$

$$\frac{\Delta E}{E_0} \ll 1,$$

$$\theta_e \ll 1, \tag{27}$$

where γ_0 and $\Delta\gamma$ are defined as $\gamma_0 = E_0/(m_e c^2)$ and $\Delta\gamma = \Delta E/(m_e c^2)$, respectively, where m_e is the electron rest mass. The average electron beam energy and its spread are defined as E_0 and ΔE, respectively. By using Eqs. (3)–(10) and Eq. (18) and the conditions in Eq. (27), the phase term defined in Eq. (21) is reduced to

$$\Phi(\boldsymbol{Q},\boldsymbol{x},\boldsymbol{x}',\Delta E) = kL + \frac{k}{2L}[(X-x)^2+(Y-y)^2] + h(\boldsymbol{Q},\boldsymbol{x},\boldsymbol{x}',\Delta E), \tag{28}$$

$$\begin{aligned} h(\boldsymbol{Q},\boldsymbol{x},\boldsymbol{x}',\Delta E) &= h(\boldsymbol{Q},\boldsymbol{x},\boldsymbol{x}') \\ &= \frac{k\rho_0(X-x-Lx')}{2L} \\ &\quad \times \left(\frac{1}{\gamma_0^2} + \frac{(X-x-Lx')^2+3(Y-y-Ly')^2}{3L^2} \right). \end{aligned} \tag{29}$$

The first two terms on the right-hand side in Eq. (28) come from a paraxial approximation, which always appears in the far-field calculation. If we consider only these terms and take G to be constant, the van Cittert–Zernike theorem in Eq. (2) is obtained. On the other hand, the third term h is the characteristic of the bending magnet radiation because this term depends on the bending radius. Since this term is the third-order, it should be much smaller than unity and can be neglected for some conditions. This term does not contain $\Delta\gamma$, which only appears in higher than third-order terms. It is noted that the third term is not symmetric with respect to x and y.

Next, we investigate the wave form G_i. In the the vertical direction, the polarization depends on the observer point. The beam profile for the π-polarization component has two peaks in the vertical direction, and the coherence cannot be easily treated [9]. In the horizontal plane, the intensity of the π-polarization component is much weaker than that of the σ-polarization component. For this reason we consider only the σ-polarization component, G_σ. Since the radiation is (not) homogeneous in the (vertical) horizontal direction, G_σ is the function of the vertical coordinate. It is well known that the beam profile of the bending magnet radiation at the far point is written with the modified Bessel function [11]. However, this function is not convenient for the analytical treatment. To overcome this, we approximate it with the Gaussian form, which is

$$G_\sigma(\boldsymbol{Q},\boldsymbol{x},\boldsymbol{x}') = G\exp\left(-\frac{(Y-y-Ly')^2}{4\bar{\sigma}_p^2} \right), \tag{30}$$

$$\bar{\sigma}_p^2 = \sigma_p^2 + L^2\sigma_p'^2, \tag{31}$$

$$\sigma_p\sigma_p' = \frac{\lambda}{4\pi}, \tag{32}$$

where σ_p, σ_p', and $\bar{\sigma}_p$ are the beam size and the beam divergence of the radiation by a single electron at the waist, and the beam size at the observer position, respectively.

III. SPATIAL COHERENCE OF BENDING MAGNET RADIATION

Since we have obtained the approximate field of the bending magnet radiation, we calculate the (first-order) spatial coherence.

The spatial coherence at $\boldsymbol{Q}_1 = (X_1, Y_1, L)$ and $\boldsymbol{Q}_2 = (X_2, Y_2, L)$ is defined as [4]

$$\gamma_{i,j}(\boldsymbol{Q}_1,\boldsymbol{Q}_2;\omega) = \frac{\Gamma_{i,j}(\boldsymbol{Q}_1,\boldsymbol{Q}_2;\omega)}{\sqrt{\Gamma_{i,i}(\boldsymbol{Q}_1,\boldsymbol{Q}_1;\omega)}\sqrt{\Gamma_{j,j}(\boldsymbol{Q}_2,\boldsymbol{Q}_2;\omega)}}, \tag{33}$$

$$\Gamma_{i,j}(\boldsymbol{Q}_1,\boldsymbol{Q}_2;\omega) = \langle E_i^*(\boldsymbol{Q}_1,\omega)E_j(\boldsymbol{Q}_2,\omega)\rangle, \tag{34}$$

where $\langle\cdots\rangle$ denotes the ensemble average with respect to the electrons parameters; i,j denote the polarization. If we use the representation of the electric field in Eqs. (20) and (23), we have

$$\begin{aligned} \Gamma_{i,j}(\boldsymbol{Q}_1,\boldsymbol{Q}_2;\omega) &= e^{-i[\chi_i(\boldsymbol{Q}_1)-\chi_j(\boldsymbol{Q}_2)]} \\ &\quad \times \langle G_i(\boldsymbol{Q}_1,\boldsymbol{x},\boldsymbol{x}')G_j(\boldsymbol{Q}_2,\boldsymbol{x},\boldsymbol{x}') \\ &\quad \times e^{-i\Phi(\boldsymbol{Q}_1,\boldsymbol{x},\boldsymbol{x}')+i\Phi(\boldsymbol{Q}_2,\boldsymbol{x},\boldsymbol{x}')}\rangle. \end{aligned} \tag{35}$$

The ensemble average can be replaced by integration with the electron phase-space density, namely,

$$\begin{aligned} \Gamma_{i,j}(\boldsymbol{Q}_1,\boldsymbol{Q}_2;\omega) &= e^{-i[\chi_i(\boldsymbol{Q}_1)-\chi_j(\boldsymbol{Q}_2)]} \\ &\quad \times \int d\boldsymbol{x}d\boldsymbol{x}'d(\Delta E)I_0(\boldsymbol{x},\boldsymbol{x}';\Delta E) \\ &\quad \times G_i(\boldsymbol{Q}_1,\boldsymbol{x},\boldsymbol{x}')G_j(\boldsymbol{Q}_2,\boldsymbol{x},\boldsymbol{x}') \\ &\quad \times e^{i[-\Phi(\boldsymbol{Q}_1,\boldsymbol{x},\boldsymbol{x}')+\Phi(\boldsymbol{Q}_2,\boldsymbol{x},\boldsymbol{x}')]} \\ &= e^{i\Psi_{i,j}(\boldsymbol{Q}_1,\boldsymbol{Q}_2)}\int d\boldsymbol{x}d\boldsymbol{x}'I(\boldsymbol{x},\boldsymbol{x}') \\ &\quad \times e^{ik(xD_x+yD_y)/L}G_i(\boldsymbol{Q}_1,\boldsymbol{x},\boldsymbol{x}') \end{aligned}$$

$$G_j(\boldsymbol{Q}_2,\boldsymbol{x},\boldsymbol{x}')e^{-ih(\boldsymbol{Q}_1,\boldsymbol{x},\boldsymbol{x}')+ih(\boldsymbol{Q}_2,\boldsymbol{x},\boldsymbol{x}')}, \tag{36}$$

where

$$D_x=X_1-X_2, \tag{37}$$

$$D_y=Y_1-Y_2, \tag{38}$$

$$\Psi_{i,j}(\boldsymbol{Q}_1,\boldsymbol{Q}_2)=\frac{k(X_2^2-X_1^2+Y_2^2-Y_1^2)}{2L}-\chi_i(\boldsymbol{Q}_1)+\chi_j(\boldsymbol{Q}_2), \tag{39}$$

and Eq. (28) is used. Since $\Psi_{i,j}$ does not depend on the integration variables $\boldsymbol{x}$ and $\boldsymbol{x}'$, it does not affect the coherence. $I_0(\boldsymbol{x},\boldsymbol{x}';\Delta E)$ is the five-dimensional phase-space density of the electron beam, and we defined

$$I(\boldsymbol{x},\boldsymbol{x}')=\int d(\Delta E)I_0(\boldsymbol{x},\boldsymbol{x}';\Delta E). \tag{40}$$

To investigate the phase terms in the integration in Eq. (36), it is convenient to define the phase difference as

$$h(\boldsymbol{Q}_1,\boldsymbol{x},\boldsymbol{x}')-h(\boldsymbol{Q}_2,\boldsymbol{x},\boldsymbol{x}')=h_0(\boldsymbol{Q}_1,\boldsymbol{Q}_2)+\delta h(\boldsymbol{Q}_1,\boldsymbol{Q}_2,\boldsymbol{x}_L), \tag{41}$$

where

$$\boldsymbol{x}_L\equiv\boldsymbol{x}+L\boldsymbol{x}', \tag{42}$$

$$h_0(\boldsymbol{Q}_1,\boldsymbol{Q}_2)=h(\boldsymbol{Q}_1,\boldsymbol{0},\boldsymbol{0})-h(\boldsymbol{Q}_2,\boldsymbol{0},\boldsymbol{0}), \tag{43}$$

$$\begin{aligned}\delta h(\boldsymbol{Q}_1,\boldsymbol{Q}_2,\boldsymbol{x}_L)=\frac{k\rho_0}{2L^3}\{&D_x x_L^2+D_x y_L^2+2D_y x_L y_L\\&-[(x_1+x_2)D_x+(y_1+y_2)D_y]x_L\\&-[(x_1+x_2)D_y+(y_1+y_2)D_x]y_L\}.\end{aligned} \tag{44}$$

It is noted that h_0 does not contain $\boldsymbol{x}$ and $\boldsymbol{x}'$ and does not affect the visibility. Using Eqs. (30), (36), and (41), the coherence of the σ-polarization component is reduced to

$$\begin{aligned}\Gamma_{\sigma,\sigma}(\boldsymbol{Q}_1,\boldsymbol{Q}_2;\omega)=|G|^2e^{i\Psi_{\sigma,\sigma}(\boldsymbol{Q}_1,\boldsymbol{Q}_2)-ih_0(\boldsymbol{Q}_1,\boldsymbol{Q}_2)}\int d\boldsymbol{x}d\boldsymbol{x}'I(\boldsymbol{x},\boldsymbol{x}')e^{ik(xD_x+yD_y)/L-i\delta h(\boldsymbol{Q}_1,\boldsymbol{Q}_2,x+Lx')}\\\times\exp\left(-\frac{(Y_1-y-Ly')^2+(Y_2-y-Ly')^2}{4\sigma_p^2}\right).\end{aligned} \tag{45}$$

Equation (45) is the basic equation for our formula.

A. Phase space of electron beam

The integration in Eq. (45) can be performed if we suppose that the electron phase-space density is Gaussian, which is

$$\begin{aligned}I_0(\boldsymbol{x},\boldsymbol{x}';\Delta E)=I_0(\boldsymbol{0},\boldsymbol{0};0)\exp\left(-\frac{\gamma_y y^2+2\alpha_y yy'+\beta_y y'^2}{2\varepsilon_y}-\frac{(\Delta E)^2}{2(\Delta E_0)^2}\right)\\\times\exp\left(-\frac{\gamma_{0x}\left(x-\eta\frac{\Delta E}{E_0}\right)^2+2\alpha_{0x}\left(x-\eta\frac{\Delta E}{E_0}\right)\left(x'-\eta'\frac{\Delta E}{E_0}\right)+\beta_{0x}\left(x'-\eta'\frac{\Delta E}{E_0}\right)^2}{2\varepsilon_{0x}}\right),\end{aligned} \tag{46}$$

where α_{x0}, β_{x0}, γ_{x0}, and ε_{0x} are the Twiss parameters and the emittance in the horizontal direction, respectively, and α_y, β_y, γ_y, and ε_y are those of the vertical direction [12]. η and η' are the horizontal dispersion and its derivative, respectively, and the vertical dispersion is assumed to be zero. After the integration in Eq. (40), we have

$$\begin{aligned}I(\boldsymbol{x},\boldsymbol{x}')=I(\boldsymbol{0},\boldsymbol{0})\exp\left(-\frac{\gamma_x x^2+2\alpha_x xx'+\beta_x x'^2}{2\varepsilon_x}\right.\\\left.-\frac{\gamma_y y^2+2\alpha_y yy'+\beta_y y'^2}{2\varepsilon_y}\right),\end{aligned} \tag{47}$$

where

$$\alpha_x=\frac{\alpha_{0x}-\frac{1}{\varepsilon_{0x}}\eta\eta'\left(\frac{\Delta E_0}{E_0}\right)^2}{\sqrt{1+\delta_x}}, \tag{48}$$

$$\beta_x=\frac{\beta_{0x}+\frac{1}{\varepsilon_{0x}}\left(\eta\frac{\Delta E_0}{E_0}\right)^2}{\sqrt{1+\delta_x}}, \tag{49}$$

$$\gamma_x=\frac{\gamma_{0x}+\frac{1}{\varepsilon_{0x}}\left(\eta'\frac{\Delta E_0}{E_0}\right)^2}{\sqrt{1+\delta_x}}, \tag{50}$$

$$\varepsilon_x = \varepsilon_{0x}\sqrt{1+\delta_x}, \tag{51}$$

$$\delta_x = \left(\frac{\Delta E_0}{E_0}\right)^2 \frac{(\gamma_{0x}\eta^2 + 2\alpha_{0x}\eta\eta' + \beta_{0x}\eta'^2)}{\varepsilon_{0x}}. \tag{52}$$

The beam size and divergence are given by

$$\sigma_x = \sqrt{\beta_x \varepsilon_x} = \sqrt{\beta_{0x}\varepsilon_{0x} + \left(\eta\frac{\Delta E_0}{E_0}\right)^2}, \tag{53}$$

$$\sigma_x' = \sqrt{\gamma_x \varepsilon_x} = \sqrt{\gamma_{0x}\varepsilon_{0x} + \left(\eta'\frac{\Delta E_0}{E_0}\right)^2}, \tag{54}$$

in the horizontal direction, respectively, and

$$\sigma_y = \sqrt{\beta_y \varepsilon_y}, \tag{55}$$

$$\sigma_y' = \sqrt{\gamma_y \varepsilon_y}, \tag{56}$$

in the vertical direction, respectively.

The following equations define the individual conditions for each of the horizontal and vertical directions under which the van Cittert–Zernike theorem is valid.

B. Horizontal direction

We calculate the first-order coherence at two points $\boldsymbol{Q}_1 = (D/2,0,L)$ and $\boldsymbol{Q}_2 = (-D/2,0,L)$. The coherence is defined in Eq. (33), which is

$$\gamma_{\sigma,\sigma}(\boldsymbol{Q}_1,\boldsymbol{Q}_2;\omega) = \frac{\Gamma_{\sigma,\sigma}(\boldsymbol{Q}_1,\boldsymbol{Q}_2;\omega)}{\sqrt{\Gamma_{\sigma,\sigma}(\boldsymbol{Q}_1,\boldsymbol{Q}_1;\omega)}\sqrt{\Gamma_{\sigma,\sigma}(\boldsymbol{Q}_2,\boldsymbol{Q}_2;\omega)}}, \tag{57}$$

where $\Gamma_{\sigma,\sigma}$ can be calculated with Eqs. (45) and (47). δh terms defined in Eq. (44), which is used to calculate Eq. (45), are written as

$$\delta h(\boldsymbol{Q}_1,\boldsymbol{Q}_2,\boldsymbol{x}_L) = \frac{k\rho_0}{2L^3}(Dx_L^2 + Dy_L^2), \tag{58}$$

$$\delta h(\boldsymbol{Q}_1,\boldsymbol{Q}_1,\boldsymbol{x}_L) = \delta h(\boldsymbol{Q}_2,\boldsymbol{Q}_2,\boldsymbol{x}_L) = 0. \tag{59}$$

After performing this integration and using the definition of the coherence in Eq. (57), we have

$$|\gamma_{\sigma,\sigma}(\boldsymbol{Q}_1,\boldsymbol{Q}_2;\omega)| = \sqrt[4]{\frac{\left(1+\frac{\varepsilon_y\overline{\beta}_y}{\sigma_p^2}\right)^2}{\left\{1+\left(\frac{k\rho_0 D\varepsilon_x\overline{\beta}_x}{L^3}\right)^2\right\}\left\{\left(1+\frac{\varepsilon_y\overline{\beta}_y}{\sigma_p^2}\right)^2+\left(\frac{k\rho_0 D\varepsilon_y\overline{\beta}_y}{L^3}\right)^2\right\}}} \times \exp\left[-\frac{k^2D^2\sigma_x^2}{2L^2}\left(\frac{1+\frac{\overline{\beta}_x}{\beta_x}\left(\frac{k\rho_0\varepsilon_x D}{L^2}\right)^2}{1+\left(\frac{k\rho_0\varepsilon_x\overline{\beta}_x D}{L^3}\right)^2}\right)\right], \tag{60}$$

where

$$\overline{\beta}_x = \beta_x - 2L\alpha_x + L^2\gamma_x, \tag{61}$$

$$\overline{\beta}_y = \beta_y - 2L\alpha_y + L^2\gamma_y. \tag{62}$$

$\overline{\beta}_x$ and $\overline{\beta}_y$ can be obtained by transforming β_x and β_y in the free space with distance L, respectively.

If the van Cittert–Zernike theorem is available, the coherence should be

$$|\gamma_{\sigma,\sigma}(\boldsymbol{Q}_1,\boldsymbol{Q}_2;\omega)| = \exp\left(-\frac{k^2D^2\sigma_x^2}{2L^2}\right), \tag{63}$$

which is obtained by putting $\rho_0 \to 0$ in Eq. (60). By comparing Eqs. (60) and (63), the van Cittert–Zernike theorem is available if the following are satisfied for $D = L/k\sigma_x$:

$$\frac{k\rho_0 D\varepsilon_x\overline{\beta}_x}{L^3} \ll 1, \tag{64}$$

$$\frac{k\rho_0 D\varepsilon_y\overline{\beta}_y}{L^3} \ll 1 + \frac{\varepsilon_y\overline{\beta}_y}{\sigma_p^2}, \tag{65}$$

$$\sqrt{\frac{\overline{\beta}_x}{\beta_x}}\left(\frac{k\rho_0\varepsilon_x D}{L^2}\right) \ll 1. \tag{66}$$

As a result, the following three conditions are derived to make the van Cittert–Zernike theorem valid:

$$\sigma_x \gg \frac{\rho_0\overline{\beta}_x\varepsilon_x}{L^2}, \tag{67}$$

$$\sigma_x \gg \frac{\rho_0 \overline{\beta}_y \varepsilon_y}{L^2\left(1+\frac{\overline{\beta}_y \varepsilon_y}{\overline{\sigma}_p^2}\right)}, \tag{68}$$

and

$$\sigma_x \gg \sqrt{\frac{\overline{\beta}_x}{\beta_x}}\frac{\rho_0 \varepsilon_x}{L}. \tag{69}$$

Consequently, the van Cittert–Zernike theorem is available in the horizontal direction if the three conditions in Eqs. (67), (68), and (69) are satisfied.

If L is very large, we can put $\overline{\beta}_x \simeq L^2\gamma_x, \overline{\beta}_y \simeq L^2\gamma_y$. Then Eqs. (67), (68), and (69) are written as

$$\sigma_x \gg \rho_0 \sigma_x'^2, \tag{70}$$

$$\sigma_x \gg \rho_0 \frac{\sigma_y'^2}{\left[1+\left(\frac{\sigma_y'}{\sigma_p'}\right)^2\right]}, \tag{71}$$

$$\sigma_x \gg \sqrt{\frac{\gamma_x}{\beta_x}}\rho_0 \varepsilon_x, \tag{72}$$

respectively. In general, these conditions are well satisfied for the present electron storage rings.

C. Vertical direction

Next we investigate the coherence in the vertical direction. We calculate the first-order coherence at two points $\boldsymbol{Q}_1=(0,D/2,L)$ and $\boldsymbol{Q}_2=(0,-D/2,L)$. The coherence is defined in Eq.(34). δh terms are written as

$$\delta h(\boldsymbol{Q}_1,\boldsymbol{Q}_2,\boldsymbol{x}_L)=\frac{k\rho_0}{L^3}Dx_L y_L, \tag{73}$$

$$\delta h(\boldsymbol{Q}_1,\boldsymbol{Q}_1,\boldsymbol{x}_L)=\delta h(\boldsymbol{Q}_2,\boldsymbol{Q}_2,\boldsymbol{x}_L)=0. \tag{74}$$

After performing the integration and using the definition of the coherence in Eq. (57), we have

$$|\gamma_{\sigma,\sigma}(\boldsymbol{Q}_1,\boldsymbol{Q}_2;\omega)| = \sqrt{\frac{1+\frac{\varepsilon_y\overline{\beta}_y}{\overline{\sigma}_p^2}}{1+\frac{\varepsilon_y\overline{\beta}_y}{\overline{\sigma}_p^2}+\left(\frac{k\rho_0 D}{L^3}\right)^2\varepsilon_x\varepsilon_y\overline{\beta}_x\overline{\beta}_y}} \times\exp\left[-\frac{k^2D^2\sigma_y^2}{2L^2}\right] \times\left(\frac{1+\frac{L^2\varepsilon_y^2}{\varepsilon_y\beta_y\overline{\sigma}_p^2}}{1+\frac{\varepsilon_y\overline{\beta}_y}{\overline{\sigma}_p^2}+\left(\frac{k\rho_0 D}{L^3}\right)^2\varepsilon_x\varepsilon_y\overline{\beta}_x\overline{\beta}_y}\right) -\frac{\varepsilon_y\overline{\beta}_y D^2}{8\overline{\sigma}_p^2(\overline{\sigma}_p^2+\varepsilon_y\overline{\beta}_y)}\Bigg]. \tag{75}$$

If three conditions,

$$\left(\frac{k\rho_0 D}{L^3}\right)^2\varepsilon_x\varepsilon_y\overline{\beta}_x\overline{\beta}_y \ll 1+\frac{\varepsilon_y\overline{\beta}_y}{\overline{\sigma}_p^2}, \tag{76}$$

$$\frac{L^2\varepsilon_y^2}{\varepsilon_y\beta_y\overline{\sigma}_p^2}\ll 1, \tag{77}$$

$$\frac{\varepsilon_y\overline{\beta}_y D^2}{4\overline{\sigma}_p^2(\overline{\sigma}_p^2+\varepsilon_y\overline{\beta}_y)}\ll 1, \tag{78}$$

are satisfied for $D=L/(k\sigma_y)$, we can judge that the van Cittert–Zernike theorem is available. These conditions are simply written as

$$\sigma_y \gg \frac{\rho_0}{L^2}\sqrt{\frac{\varepsilon_x\varepsilon_y\overline{\beta}_x\overline{\beta}_y}{\left(1+\frac{\varepsilon_y\overline{\beta}_y}{\overline{\sigma}_p^2}\right)}}, \tag{79}$$

$$\sigma_y \gg \frac{L\varepsilon_y}{\overline{\sigma}_p} \tag{80}$$

$$\sigma_y \gg \frac{L}{2k\overline{\sigma}_p}\sqrt{\frac{\varepsilon_y\overline{\beta}_y}{\overline{\sigma}_p^2+\varepsilon_y\overline{\beta}_y}}. \tag{81}$$

As a result, the van Cittert–Zernike theorem is available in the vertical direction if conditions (79), (80), and (81) are satisfied. It is noted that these conditions depend on the wavelength of the light, since the beam profile depends on the wavelength.

For very large L, these conditions are reduced to

$$\sigma_y \gg \rho_0 \frac{\sigma_x' \sigma_y'}{\sqrt{1+\left(\frac{\sigma_y'}{\sigma_p'}\right)^2}}, \tag{82}$$

$$\sigma_y \gg \frac{\varepsilon_y}{\sigma_p'}, \tag{83}$$

$$\sigma_y \gg \frac{\sigma_p}{\sqrt{1+\left(\frac{\sigma_p'}{\sigma_y'}\right)^2}}. \tag{84}$$

In this section we calculated the spatial coherence of the bending magnet radiation and derived some conditions under which the van Cittert–Zernike theorem can be used.

The conditions are given individually for each of the horizontal and vertical directions. It is important that in the horizontal direction, Eqs. (67) and (69) do not depend on the wavelength of light. If $\overline{\sigma_p^2} \gg \varepsilon \overline{\beta_y}$, which is easily satisfied for visible light, is satisfied, Eq. (68) also does not depend on the wavelength. This means that conditions are determined almost entirely with the electron-beam parameters and bending radius; the wave form of light has little effect on the coherence. In the vertical direction, the wave form may affect the coherence because all conditions (79), (80), and (81) depend on the wavelength. Since the Gaussian approximation is not satisfactory for the bending magnet radiation, these conditions, which are based on the Gaussian approximation, are not complete. Taking into account these circumstances, it is more reliable to use the van Cittert–Zernike theorem in the horizontal direction than in the vertical direction to estimate the electron-beam size.

The discussion in this section is based on the approximations in Eqs. (23), (28), (29), (30), and (45). To confirm that these approximations are reasonable, we calculate the spatial coherence from the first principle and compare it with the results derived in this section.

IV. NUMERICAL CALCULATIONS

In this section we calculate the spatial coherence, $|\gamma_{\sigma,\sigma}(\boldsymbol{Q}_1,\boldsymbol{Q}_2;\omega)|$, using Eqs. (12), (17), (33), and (34). Since we consider only the σ-polarization component, suffixes for the polarization are not explicitly written in this section.

First we calculate the coherence when the electron beam has some size and no divergence in the vertical and horizontal directions. The coherence can be calculated by the van Cittert–Zernike theorem in this case.

Next, we calculate the coherence when the electron beam has both small size and divergence. We show that the van Cittert–Zernike theorem is also applicable in the horizontal and vertical directions.

Last, we calculate the coherence when the electron beam has a large divergence and no size. If the van Cittert–Zernike theorem were applied, the coherence would be unity for any divergence of the electron beam. However, since the conditions derived in the last section are not satisfied, the coherence must decrease. We show that the coherence can be almost completely calculated using Eq. (60) or (75) if the vertical divergence of the electron beam is very small. If the vertical divergence is very large, the coherence can be approximately calculated because the Gaussian approximation is not a complete one.

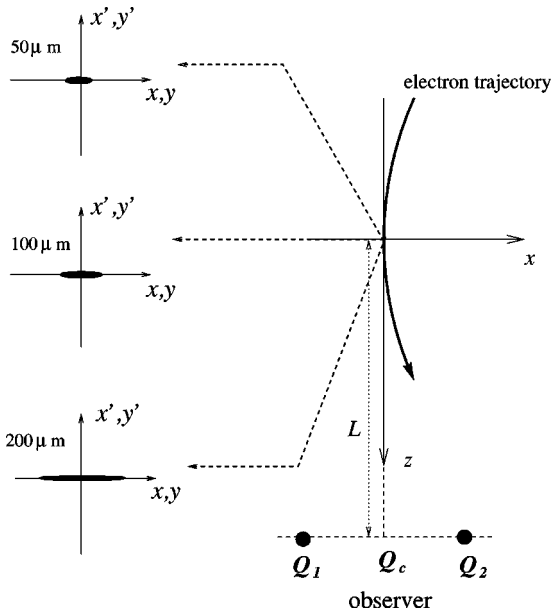

FIG. 3. Arrangement used to calculate spatial coherence for a finite beam size with no divergence.

A. Finite beam size and no beam divergence

Here, we calculate the coherence when the electron beam has some size and no divergence.

We consider the arrangement as shown in Fig. 3. Two vectors, $\boldsymbol{n}$ and $\boldsymbol{\beta}$, become parallel at the origin when the observer coordinate $\boldsymbol{Q}_c$ is at the center of two points, $\boldsymbol{Q}_1$ and $\boldsymbol{Q}_2$. For all numerical calculations in this section, we choose the distance L between the origin and $\boldsymbol{Q}_c$, the bending radius ρ_0, the wavelength of the light λ, and the electron-beam energy to be 10 m, 8.66 m, 500 nm and 2.5 GeV, respectively. We use three electron beam sizes: 50, 100, and 200 μm. The electron density $I(\boldsymbol{x},\boldsymbol{x}')$ is chosen to be

$$I(\boldsymbol{x},\boldsymbol{x}') = I(\boldsymbol{0},\boldsymbol{0}) \exp\left(-\frac{x^2}{2\sigma_x^2} - \frac{y^2}{2\sigma_y^2}\right) \delta(\boldsymbol{x}'). \tag{85}$$

This can be obtained by taking the following limit in Eq. (47):

$$\sqrt{\beta_{x,y}\varepsilon_{x,y}} \to \sigma_{x,y},$$

$$\sqrt{\gamma_{x,y}\varepsilon_{x,y}} \to 0,$$

$$\varepsilon_{x,y} \to 0.$$

If the van Cittert–Zernike theorem can be applied, the spatial coherence should be given by

$$|\gamma_{\sigma,\sigma}(\boldsymbol{Q}_1,\boldsymbol{Q}_2;\omega)| = \exp\left(-\frac{D_x^2}{8\sigma_{cx}^2} - \frac{D_y^2}{8\sigma_{cy}^2}\right), \tag{86}$$

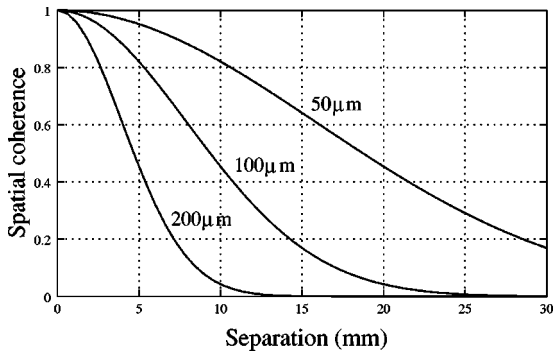

FIG. 4. Spatial coherence in the horizontal direction with a horizontal beam size.

where the coherent size σ_{cx} and σ_{cy} in the horizontal and vertical directions are defined as

$$\sigma_{cx}=\frac{L\lambda}{4\pi\sigma_x}, \tag{87}$$

$$\sigma_{cy}=\frac{L\lambda}{4\pi\sigma_y}, \tag{88}$$

respectively. For consideration of the horizontal direction, we put $\boldsymbol{Q}_1=(D/2,0,L)$, $\boldsymbol{Q}_2=(-D/2,0,L)$, and $\sigma_y=0$, and for the vertical direction we put $\boldsymbol{Q}_1=(0,D/2,L)$, $\boldsymbol{Q}_2=(0,-D/2,L)$, and $\sigma_x=0$.

The results of numerical calculations are shown in Figs. 4 and 5 and Table I. In Fig. 4 and Fig. 5, the absolute values of the spatial coherence are plotted as a function of the separation of two observer points D in the horizontal and vertical directions, respectively. The curves of the spatial coherence are almost the same in both directions. By fitting these curves with the Gaussian shape defined in Eq. (86), we obtain the coherent size numerically and compare this with the coherent size given by the van Cittert–Zernike theorem in Eqs. (87) and (88). The van Cittert–Zernike theorem gives the same results as the numerical calculations, so that this theorem is available in the vertical and horizontal directions.

Theoretically, the van Cittert–Zernike theorem can be applied for any beam size. However, it is quite difficult to measure a very small size in the vertical direction. If the vertical size σ_y is very small, the separation D, which must be larger than the coherent size $2\sigma_{cy}$ defined in Eq. (88), can be very large. Since the intensity of light decreases rapidly

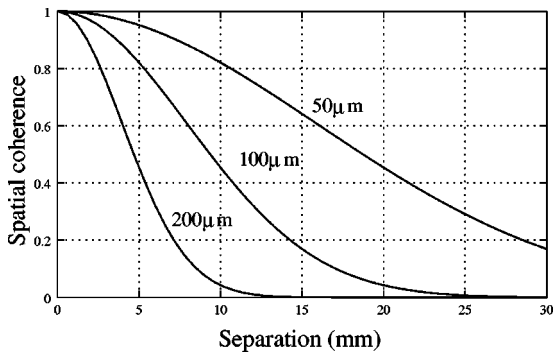

FIG. 5. Spatial coherence in the vertical direction with a vertical beam size.

TABLE I. Comparison of the coherent size for a finite electron-beam size. The coherent size calculated by the van Cittert–Zernike theorem and numerical calculation in the horizontal and vertical directions are compared.

Electron-beam size (μm)	van Cittert–Zernike Theorem (mm)	Numerical calculation Horizontal (mm)	Vertical (mm)
50	7.958	7.958	7.958
100	3.979	3.979	3.979
200	1.989	1.989	1.989

for $D/2>L\sigma_p'$ in the vertical direction, where $L\sigma_p'$ is the beam size of the light at the observer point, the light itself is too weak to be measured accurately. Therefore, in order to obtain enough light intensity, the coherent size σ_{cy} must be smaller than $L\sigma_p'$. Using Eqs. (87) and (32), we have another condition,

$$\sigma_y>\sigma_p. \tag{89}$$

B. Small beam size and beam divergence

Next, we consider an electron beam with finite size and divergence. We consider the arrangement as shown in Fig. 6.

For a simplicity, the electron density $I(\boldsymbol{x},\boldsymbol{x}')$ is chosen to be

$$I(\boldsymbol{x},\boldsymbol{x}')=I(\boldsymbol{0},\boldsymbol{0})\exp\left(-\frac{x^2}{2\sigma_x^2}-\frac{y^2}{2\sigma_y^2}\right)\delta(\boldsymbol{x}'-s\boldsymbol{x}), \tag{90}$$

where s is a constant and we take it to be 1 (1/m) here. This can be obtained by taking the following limit in Eq. (47):

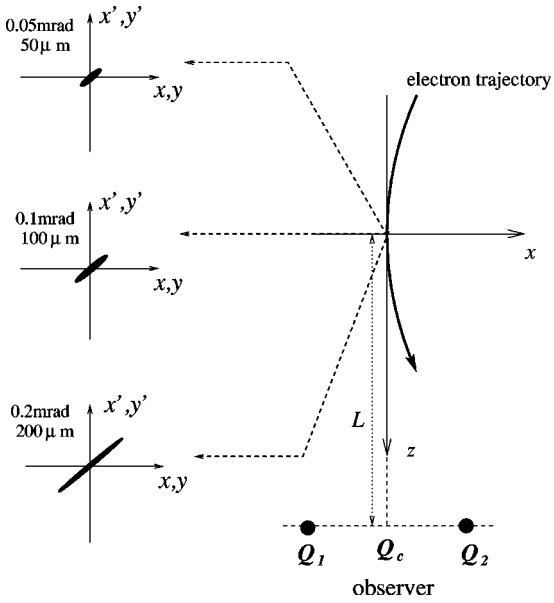

FIG. 6. Arrangement used to calculate the spatial coherence for a small beam divergence and small beam size.

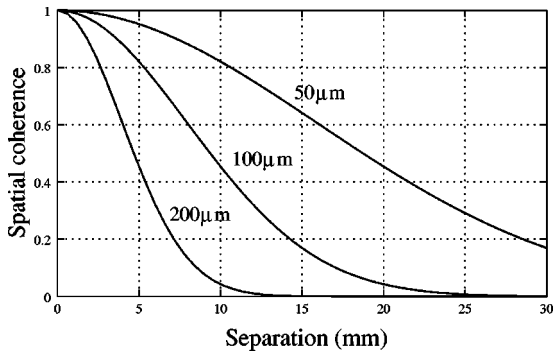

FIG. 7. Spatial coherence in the horizontal direction with a horizontal beam size and divergence.

$$\sqrt{\beta_{x,y}\varepsilon_{x,y}}\rightarrow\sigma_{x,y},$$

$$\sqrt{\gamma_{x,y}\varepsilon_{x,y}}\rightarrow\sigma'_{x,y}=|s|\sigma_{x,y},$$

$$\varepsilon_{x,y}\rightarrow 0.$$

In this case, the coherent size expected by the van Cittert–Zernike theorem is also given in Eqs. (87) and (88). We choose three parameters for $\sigma_{x,y}$, which are 50 μm, 100 μm, and 200 μm. For these parameters, the electron-beam divergences $\sigma'_{x,y}$ are set to be 0.05 mrad, 0.1 mrad, and 0.2 mrad, respectively, and all conditions derived in the last section are well satisfied. In the same way as the previous case, for consideration of the horizontal direction, we set $\boldsymbol{Q}_1=(D/2,0,L)$, $\boldsymbol{Q}_2=(-D/2,0,L)$, and $\sigma_y=0$, $\sigma'_y=0$, and for the vertical direction we set $\boldsymbol{Q}_1=(0,D/2,L)$, $\boldsymbol{Q}_2=(0,-D/2,L)$, and $\sigma_x=0$, $\sigma'_x=0$.

The results of numerical calculations are shown in Figs. 7 and 8 and Table II. In Fig. 7 and Fig. 8 the spatial coherence is plotted as a function of the separation of two observer points D in the horizontal and the vertical directions, respectively. The van Cittert–Zernike theorem and the numerical calculation agree for the coherent size. Very little discrepancy in the vertical direction is due to the fact that the radiation is not homogeneous in this direction. In any case, the spatial coherence is almost entirely determined by the electron-beam size and does not depend on the electron-beam divergence. Therefore, even if the electron beam has both beam size and beam divergence, the van Cittert–Zernike theorem is a good approximation with which to calculate the coherent size, as long as the conditions are satisfied.

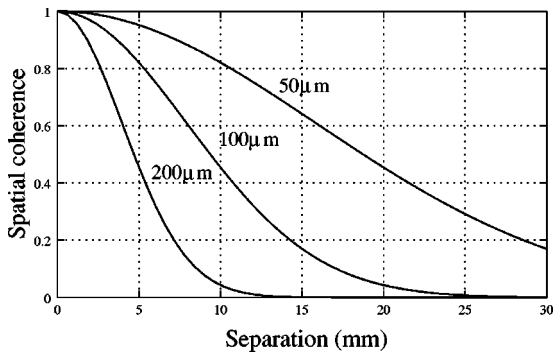

FIG. 8. Spatial coherence in the vertical direction with a vertical beam size and divergence.

TABLE II. Comparison of the coherent size for a small electron-beam size and divergence. The coherent size calculated by the van Cittert–Zernike theorem and numerical calculation in the horizontal and vertical directions are compared.

Electron-beam size (μm)	van Cittert–Zernike Theorem (mm)	Numerical calculation Horizontal (mm)	Vertical (mm)
50	7.958	7.958	7.961
100	3.979	3.979	3.982
200	1.989	1.989	1.991

As in the previous case, there is a condition at divergence of the light beam under which the light beam reaches the observer points with sufficient intensity. In this case, the size of the light beam at the observer point is $L\sqrt{\sigma_p'^2+\sigma_y'^2}$ in the vertical direction. Therefore, the minimum size of the electron beam to be measured in the vertical direction is given by the inequality

$$\sigma_y>\frac{\sigma_p}{\sqrt{1+\left(\dfrac{\sigma'_y}{\sigma'_p}\right)^2}}, \tag{91}$$

where Eq. (32) is used. It is noted this condition is different from Eq. (84).

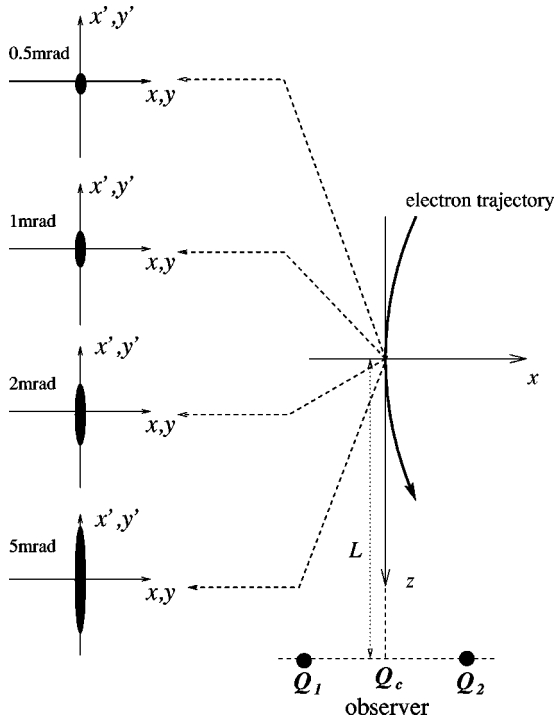

FIG. 9. Arrangement used to calculate the spatial coherence for a finite large divergence with no beam size at the origin.

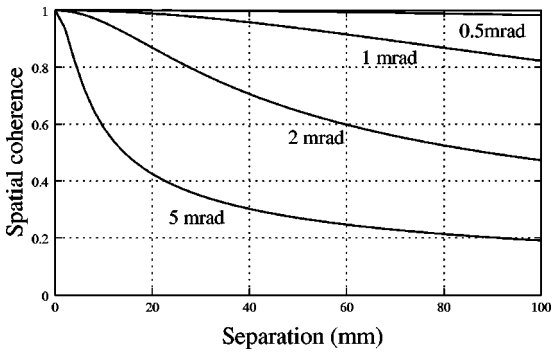

FIG. 10. Spatial coherence in the horizontal direction with horizontal divergence.

C. Large beam divergence

Finally, we calculate the coherence when the electron beam has a large divergence and no beam size at the origin. The arrangement is shown in Fig. 9.

We calculate four cases. For each case we use four electron-beam divergences: 0.5, 1, 2, and 5 mrad. The distribution of electron beam is put as

$$I(\boldsymbol{x},\boldsymbol{x}')=I(\boldsymbol{0},\boldsymbol{0})\exp\left(-\frac{x'^2}{2\sigma_x'^2}-\frac{y'^2}{2\sigma_y'^2}\right)\delta(\boldsymbol{x}). \qquad (92)$$

This can be obtained by taking the following limit in Eq. (47):

$$\sqrt{\beta_{x,y}\varepsilon_{x,y}}\to 0,$$

$$\sqrt{\gamma_{x,y}\varepsilon_{x,y}}\to\sigma'_{x,y},$$

$$\varepsilon_{x,y}\to 0.$$

It is noted that if the van Cittert–Zernike theorem is available, the coherence must be unity for any case.

1. Horizontal divergence → horizontal coherence

We use the parameters,

$$\boldsymbol{Q}_1=\left(\frac{D}{2},0,L\right),\quad \boldsymbol{Q}_2=\left(-\frac{D}{2},0,L\right),\quad \sigma'_x\neq 0,\sigma'_y=0.$$

The coherence curves calculated numerically are shown in Fig. 10. We see that the curves are not Gaussian in shape,

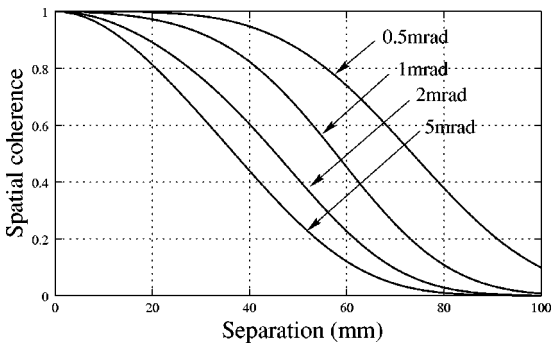

FIG. 11. Spatial coherence in the vertical direction with vertical divergence.

TABLE III. Comparison of the coherent size for a large electron-beam divergence in the vertical direction. The coherent size expected by Eq. (95) and the numerical calculation are compared.

Electron-beam divergence (mrad)	Analytical calculation (mm)	Numerical calculation (mm)
0.5	66.6	31.2
1	36.7	23.0
2	24.0	18.1
5	19.8	15.2

although the divergence distribution of the electron beam is Gaussian. This comes from the third-order contribution of the phase. Actually, these curves are fitted exactly with the curves expected analytically in Eq. (60), which is

$$|\gamma_{\sigma,\sigma}(\boldsymbol{Q}_1,\boldsymbol{Q}_2;\omega)|=\frac{1}{\sqrt[4]{1+\left(\frac{k\rho_0 D\varepsilon_x\overline{\beta}_x}{L^3}\right)^2}}, \qquad (93)$$

where $\varepsilon_x\overline{\beta}_x=L^2\sigma_x'^2$ in this case.

2. Vertical divergence → vertical coherence

We use the parameters

$$\boldsymbol{Q}_1=\left(0,\frac{D}{2},L\right),\quad \boldsymbol{Q}_2=\left(0,-\frac{D}{2},L\right),\quad \sigma'_x=0,\sigma'_y\neq 0.$$

The results of numerical calculations are shown in Fig. 11. The coherence decreases more rapidly than that of the first case (horizontal divergence → horizontal coherence). Moreover, the curves are similar to the Gaussian shape.

According to Eq. (75), the coherent size is given by

$$|\gamma_{\sigma,\sigma}(\boldsymbol{Q}_1,\boldsymbol{Q}_2;\omega)|=\exp\left(-\frac{\varepsilon_y\overline{\beta}_y D^2}{8\overline{\sigma}_p^2(\overline{\sigma}_p^2+\varepsilon_y\overline{\beta}_y)}\right)$$

$$=\exp\left(-\frac{D^2}{8\sigma_c^2}\right), \qquad (94)$$

where

$$\sigma_c=\sqrt{\frac{\overline{\sigma}_p^2(\overline{\sigma}_p^2+\varepsilon_y\overline{\beta}_y)}{\varepsilon_y\overline{\beta}_y}}. \qquad (95)$$

In this case, we can put $\varepsilon_y\overline{\beta}_y=L^2\sigma_y'^2$ and $\sigma'_p=1.79$ mrad. As shown in Table III, we compare this with the coherent size calculated numerically, which is obtained by fitting the curves in Fig. 11 by Eq. (94). A large discrepancy is found, especially for the large coherent size, which comes from the fact that the bending magnet radiation is not exactly the Gaussian beam. Therefore, the Gaussian approximation is not perfect for calculating coherence and in order to confirm precisely whether the van Cittert–Zernike theorem can be used in the vertical direction, numerical calculation for each specific case is necessary.

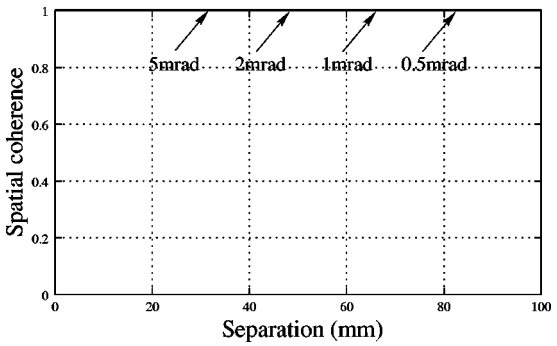

FIG. 12. Spatial coherence in the vertical direction with horizontal divergence.

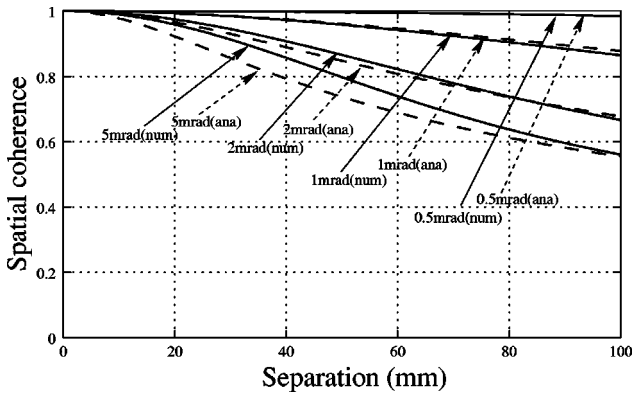

FIG. 13. Spatial coherence in the horizontal direction with vertical divergence. ''num'' and ''ana'' represent the numerical calculation and the analytical calculation, respectively.

3. Horizontal divergence → vertical coherence

We use the parameters

$$\boldsymbol{Q}_1=\left(0,\frac{D}{2},L\right),\quad \boldsymbol{Q}_2=\left(0,-\frac{D}{2},L\right),\quad \sigma_x'\neq 0,\sigma_y'=0.$$

The results of numerical calculations are shown in Fig. 12. The coherence is always unity in this case, as expected from Eq. (75), because there is no phase difference between two observer points at all. Moreover, the intensities at two points are always the same. Therefore, the horizontal divergence of the electron beam does not affect the vertical coherence at all.

4. Vertical divergence → horizontal coherence

We use the parameters

$$\boldsymbol{Q}_1=\left(\frac{D}{2},0,L\right),\quad \boldsymbol{Q}_2=\left(-\frac{D}{2},0,L\right),\quad \sigma_x'=0,\sigma_y'\neq 0.$$

According to Eq. (60), the expected curve is

$$|\gamma_{\sigma,\sigma}(\boldsymbol{Q}_1,\boldsymbol{Q}_2;\omega)|=\sqrt[4]{\frac{\left(1+\frac{\varepsilon_y\overline{\beta}_y}{\overline{\sigma}_p^2}\right)^2}{\left(1+\frac{\varepsilon_y\overline{\beta}_y}{\overline{\sigma}_p^2}\right)^2+\left(\frac{k\rho_0 D\varepsilon_y\overline{\beta}_y}{L^3}\right)^2}},\tag{96}$$

where $\varepsilon_y\overline{\beta}_y=L^2\sigma_y'^2$ in this case. The results of numerical calculations and the analytically expected curves in Eq.(96) are shown in Fig. 13. We can see that Eq. (96) is not a complete approximation to describe the coherence. This shows that the Gaussian approximation is a poor approximation with which to calculate the coherence again.

V. SUMMARY

We calculated the spatial coherence of the bending magnet radiation while assuming that the radiation is represented with the phase Φ and the wave form $\boldsymbol{G}$. The result was compared with a numerical calculation.

We showed that the van Cittert–Zernike theorem can be applied in the horizontal and vertical directions if the electron-beam size is much larger than a certain value σ_e so that the electron-beam size can be estimated by measuring the spatial coherence. On the other hand, if the electron-beam size is much smaller than σ_e, the electron-beam divergence can be estimated by measuring the spatial coherence. The conditions under which the van Cittert–Zernike theorem is valid are written in Eqs. (67), (68), and (69) for the horizontal direction and in Eqs. (79), (80), and (81) for the vertical direction. If the vertical divergence of the electron beam is small, σ_e in the horizontal direction is fully determined by the bending radius and the electron-beam parameters. For the vertical direction, σ_e depends heavily on the wavelength of light as well as on the bending radius and the electron-beam parameters. It is complicated to justify the applicability of the van Cittert–Zernike theorem in the vertical direction. In that sense, an estimation of the vertical size is more difficult than that of the horizontal size. However, we can easily eliminate this difficulty by introducing a vertical bending magnet and exchanging the characteristics of measurement in the horizontal direction and the vertical direction. A series of numerical calculations based on the first principles were carried out for some specific cases to make the argument clear.

We emphasize some advantages of the SR interferometer in measuring the emittance compared to other optical methods, such as via the x-ray pinhole camera [13–15]. We can measure the electron-beam size by the degree to which the SR interferometer is affected by the field depth and the diffraction. These effects are already included in the principle of the measurement as explained in this paper. Also, we can choose any wavelength for the measurement, especially in the horizontal direction, so long as the interference pattern can be measured, although the visible light has some technical advantages in treating the optical system and detector easily. The accuracy of the measurement of emittance is limited only by the errors of the optical system, such as the deformation and blot of the mirror, and the resolution of the charge-coupled device camera to measure the interference pattern.

[1] T. Mitsuhashi, in *Proceedings of the 1997 Particle Accelerator Conference, Vancouver, B.C., 1997*, edited by Martin Comyn (IEEE, Piscataway, NJ, 1998), p. 766.
[2] F. Zernike, Physica (Amsterdam) **5**, 785 (1938).
[3] P. H. van Cittert, Physica (Amsterdam) **1**, 201 (1934).
[4] M. Born and E. Wolf, *Principle of Optics*, 6th ed. (Pergamon Press, New York, 1980).
[5] J. Schwinger, Phys. Rev. **75**, 1912 (1949).
[6] K. J. Kim, Nucl. Instrum. Methods Phys. Res. A **246**, 71 (1986).
[7] R. Coisson, Appl. Opt. **34**, 904 (1995).
[8] N. Y. Smolyakov, Nucl. Instrum. Methods Phys. Res. A **405**, 229 (1998).
[9] Y. Takayama, T. Hatano, T. Miyahara, and W. Okamoto, J. Synchrotron Radiat. **5**, 1187 (1998).
[10] G. A. Schott, *Electromagnetic Radiation* (Cambridge University Press, Cambridge, England, 1912).
[11] J. D. Jackson, *Classical Electrodynamics* (Wiley, New York, 1962).
[12] E. D. Courant and H. S. Snyder, Ann. Phys. (N.Y.) **3**, 1 (1958).
[13] G. P. Jackson, R. H. Siemann, D. N. Mills, in *Proceedings of the 12th Conference on High Energy Accelerators, Batavia, 1983*, edited by Francis T. Cola and Rene Donaldson (Fermi Laboratory, Batavia, 1983), p. 217.
[14] A. Ogata, T. Mitsuhashi, T. Katsura, N. Yamamoto, and T. Kawamoto, in *Proceedings of the 1989 IEEE Particle Accelerator Conference, Chicago, 1989*, edited by Floyd Bennet and Joyce Kopta (IEEE, New York, 1989), p. 1498.
[15] P. Elleaume, C. Fortgang, C. Penel, and E. Tarazona, J. Synchrotron Radiat. **2**, 209 (1995).